Development of an efficient 2D MCSEM inversion algorithm

*Rahul Dehiya**
Department of Earth and Climate Science, Indian Institute of Science Education and Research (IISER) Pune

rahul.dehiya@iiserpune.ac.in

Keywords

CSEM inversion, VTI, Space domain, Troll field

Abstract

This study presents a novel technique for modeling marine controlled-source electromagnetic data for 2D models. The algorithm uses a space domain approach to solve the governing Helmholtz equation. Therefore, it does not require the inverse Fourier transform to obtain the space domain data, as is the case for conventional wavenumber domain algorithms. An inverse modeling code is developed utilizing the proposed forward modeling algorithm. The Troll field data is used to analyze the developed code's versatility.

Introduction

The 3D nature of the source in a marine Controlled-Source ElectroMagnetic (MCSEM) method is assumed to be the chief reason for less emphasis on the development of 2D MCSEM inversion algorithms (Constable, 2010). Nonetheless, Weiss and Constable (2006) reasoned that MCSEM data recorded along a profile can be investigated using 2D MCSEM inversion algorithms. The usual MCSEM data observed at inline receivers configuration using an electric dipole is typically sensitive to the subsurface between the source and receivers (Weiss and Constable, 2006; Constable, 2010). In hydrocarbon exploration studies, the inline electric field observed over a thin buried resistive reservoir usually fit well with MCSEM data modeled by a 2D code (Key, 2016). 2D inversion can be very useful in towed MCSEM systems (Anderson and Mattsson, 2010; Constable et al., 2016), where the transmitter and receives are commonly moved along a line. Accordingly, the thousands of transmitter and receiver positions in a towed MCSEM design cause 3D inversion to be computationally costly. Further, the subsurface conductivity estimated utilizing a 2D inversion code can also be used as an initial guess for 3D inversion, reducing the cost of 3D inversion (Key, 2016). Thus, several 2D inversion codes have been written in the past (Abubakar et al., 2008; Key, 2016). The 2D MCSEM inversion has been used in numerous investigations as documented in the publications (Christine et al., 2021; Weitemeyer et al., 2010).

The computational intricacy of 2D frequency-domain forward modeling in the presence of a controlled source is the main reason for less focus on 2D inversion code than to plane-wave sources such as magnetotelluric. To overcome the 3D character of the source in a computationally efficient fashion, typically, the 2D frequency-domain MCSEM simulation is done in the wavenumber domain. For accurate space-domain responses, wavenumber-domain modeling is needed for tens of wavenumbers. For example, The MARE2DEM code uses 30 wavenumbers (Key and Ovall, 2011) followed by hundreds of thousands of Fourier transforms. In the case of inversion, the simulations must be done for both forward and adjoint fields. For example, a sensitivity matrix corresponding to m parameter and n data would require mn inverse Fourier transforms (Key, 2016). Therefore, inverse Fourier transform requirements make 2D CSEM inversion code writing challenging and computationally costly.

This study uses a space-domain forward modeling strategy to create an efficient 2D CSEM inversion algorithm. The presented algorithm is straightforward to develop. The numerical experimentations are done using Troll field data to establish the robustness of the created algorithm.

Theory

Maxwell's equations are the governing equations for modeling the marine controlled-source electromagnetic (MCSEM) data. Generally, it is preferred to recast these equations for the electric field

Development of an efficient 2D MCSEM inversion algorithm

by eliminating the magnetic field leading to the Helmholtz equation. The MCSEM data is generally analyzed in the frequency domain. Therefore, assuming $e^{-\iota\omega t}$ time dependency, the Helmholtz equation in the frequency domain can be expressed as,

$$\nabla \times \nabla \times \mathbf{E} - (\iota\omega\mu\hat{\sigma} + \omega^2\mu\epsilon)\mathbf{E} = \mathbf{s}(\omega)\delta(\boldsymbol{r} - \boldsymbol{r}_s), \quad (1)$$

where $\mathbf{E}$ denotes electric field; ω is angular frequency; μ and ϵ represent magnetic permeability and electric permittivity, respectively; $\iota = \sqrt{-1}$; $\hat{\sigma}$ denotes conductivity tensor; $\mathbf{s}(\omega)$ is the source term that can be an electric or magnetic transmitter; $\boldsymbol{r}_s = [x_s, y_s, z_s]$, is the source's position vector and δ is Dirac delta function. For anisotropy model, considering a vertical transverse isotropy (VTI) media, the $\hat{\sigma}$, is defined as,

$$\hat{\sigma} = \begin{pmatrix} \sigma_h & 0 & 0 \\ 0 & \sigma_h & 0 \\ 0 & 0 & \sigma_v \end{pmatrix} \quad (2)$$

where σ_h and σ_v represent the electric conductivity in horizontal and vertical direction, respectively. The vector equation 1 can be decomposed into three scalar equations. Considering a 2D-VTI model with strike in the y-direction, these scalar equations can be transformed in the wavenumber domain (considering $e^{\iota k_y y}$ space dependency) as,

$$\iota k_y \frac{\partial E_y}{\partial x} + \frac{\partial^2 E_z}{\partial x \partial z} + k_y^2 E_x - \frac{\partial^2 E_x}{\partial z^2} - \iota\omega\mu\sigma_h E_x = s_x(\omega)e^{\iota k_y (y - y_s)}\delta(x - x_s)\delta(z - z_s)\,, \quad (3)$$

$$\iota k_y \frac{\partial E_x}{\partial x} + \iota k_y \frac{\partial E_z}{\partial z} - \frac{\partial^2 E_y}{\partial x^2} - \frac{\partial^2 E_y}{\partial z^2} - \iota\omega\mu\sigma_h E_y = s_y(\omega)e^{\iota k_y (y - y_s)}\delta(x - x_s)\delta(z - z_s)\,, \quad (4)$$

$$\frac{\partial^2 E_x}{\partial x \partial z} + \iota k_y \frac{\partial E_y}{\partial z} - \frac{\partial^2 E_x}{\partial x^2} + k_y^2 E_z - \iota\omega\mu\sigma_v E_z = s_z(\omega)e^{\iota k_y (y - y_s)}\delta(x - x_s)\delta(z - z_s)\,, \quad (5)$$

Equations 3-5 are solved by enforcing the homogeneous Dirichlet boundary conditions (BCs) to suppress the reflection from boundaries. Now, we use these equations to analyse the symmetric and anti-symmetric nature of EM field due to electric dipole pole source at plane $y = y_s$, for 2D models. It is achievable because, at $y = y_s$, the source terms do not depend on k_y. For example, in case of a horizontal electric dipole (HED) oriented in the x-direction, the source terms in equations 4 & 5 will become zero. Furthermore, substituting $k_y = k_y$ and $E_y = -E_y$ will deliver the same set of equations. Therefore, in case of HED aliened in x-direction, the E_x and E_z components are symmetric function while E_y is an anti-symmetric function about $y = y_s$ plane; hence, we can define a BCs as,

$$E_x^{y_s^-} = E_x^{y_s^+}; E_y^{y_s^-} = -E_y^{y_s^+}; E_z^{y_s^-} = E_z^{y_s^+} \quad (6)$$

Now suppose a HED is oriented in the y-direction; the source terms of equations 3 & 5 will be zero. Again substituting $k_y = -k_y$ and $y = y_s$ in equations 3-5 provide to the following BCs;

$$E_x^{y_s^-} = -E_x^{y_s^+}; E_y^{y_s^-} = E_y^{y_s^+}; E_z^{y_s^-} = -E_z^{y_s^+} \quad (7)$$

Following the same reasoning, the BCs for vertical electric dipole (VED) can be acquired, which will be identical to Equation 6.

I propose calculating the 2D MCSEM forward modeling response in the space domain using these BCs at plane $y = y_s$ discussed above and homogeneous Dirichlet BCs for all other model sides. Notably, the system matrix depends on BCs and will not be identical for distinct transmitter types having different BCs. Thus, a source with an orientation that needs to be represented by a linear combination of diverse source types will require independent calculations. Nevertheless, in a typical MCSEM survey, the receivers are rotated to the towline direction. Again, the reciprocity principle is used to reverse the role of receivers as transmitters for efficient calculations. Since BCs are identical for a vertical and horizontal electric dipole, oriented perpendicular to the strike direction, hence, the system matrix for any arbitrarily-orientated electric dipole in a plane perpendicular to the strike direction will be identical. The present study uses a staggered-grid finite-difference technique to solve the governing equation with BCs examined above. A primary/secondary technique is utilized to manage the

source singularity. It is observed that the developed scheme needs only a few grids in the y-direction. The space in y-direction must only be discretized on any one side of the plane $y = y_s$. Now I discuss the inversion algorithm.

Inverse modeling is an optimization problem that strives to minimize the misfit between observed data, $\mathbf{d}^{obs}$, and predicted data, $\mathbf{F(m)}$. The objective function that I seek to minimize is described as,

$$\phi = ||\mathbf{W}_\mathrm{d}(\mathbf{d^{obs}} - \mathbf{F(m)})||_2 + \lambda(\alpha \left|\left|\mathbf{m} - \mathbf{m}_{ref}\right|\right|_2 + (1-\alpha)\left|\left|\mathbf{Rm}\right|\right|_2 + \beta\left|\left|\mathbf{Lm}\right|\right|_2), \quad (8)$$

where $\mathbf{W}_\mathrm{d}$, represents data covariance matrix; λ denotes regularization parameter; $\mathbf{R}$ and $\mathbf{m}_{ref}$ is Laplacian operator and reference model, respectively; $\alpha = [0,1]$; $\mathbf{L}$ is an operator that seeks to minimize the difference between horizontal and vertical conductivities (see Key, 2016) and β is a real scalar. The last term is relevant only in the case of anisotropic inversion. Employing the Gauss-Newton approach, we can write an expression for computation of correction in model parameter, $\delta\mathbf{m}_i$, at i^{th} iteration as,

$$\mathbf{H}_{i-1}\delta\mathbf{m}_\mathrm{i} = -\mathbf{g}_{i-1}, \quad (9)$$

here,

$$\mathbf{H}_{i-1} = \mathbf{J}_{i-1}^\mathrm{T}\,\mathbf{W}_\mathrm{d}^\mathrm{T}\mathbf{W}_\mathrm{d}\mathbf{J}_{i-1} + \boldsymbol{\lambda}_{i-1}(\alpha\mathbf{I}+(1\text{-}\alpha)\mathbf{R}^T\mathbf{R}+\beta\mathbf{L}^T\mathbf{L}) \quad (10)$$

and

$$\mathbf{g}_{i-1} = -\mathbf{J}_{i-1}^\mathrm{T}\,\mathbf{W}_\mathrm{d}^\mathrm{T}\mathbf{W}_\mathrm{d}(\mathbf{d}^\mathrm{obs} - \mathbf{F}(\mathbf{m}_{i-1})) + \boldsymbol{\lambda}_{i-1}(\alpha\mathbf{m}_\mathrm{ref}+(1\text{-}\alpha)\mathbf{R}^T\mathbf{R}\mathbf{m}_{i-1}+\beta\mathbf{L}^T\mathbf{L}\mathbf{m}_{i-1}) \quad (11)$$

where $\mathbf{H}_{i-1}$ and $\mathbf{g}_{i-1}$ denote Hessian and gradient of objective function calculated for the model parameter, $\mathbf{m}_{i-1}$ after $i-1^{th}$ iteration and $\mathbf{J}_{i-1}$, is the Jacobian matrix. An adjoint technique (McGillivray et al., 1994) is employed for Jacobian matrix calculation. Finally, the updated model parameter after i^{th} iteration is computed as, $\mathbf{m_i} = \mathbf{m}_{i-1} + \delta\mathbf{m}_i$. Equation 9 can be rearranged for direct estimation of the updated model parameter as,

$$\mathbf{H}_{i-1}\mathbf{m}_i = -\mathbf{g}_{i-1} + \mathbf{H}_{i-1}\mathbf{m}_{i-1}. \quad (12)$$

A normalize RMS (nRMS), defined as,

$$\mathrm{nRSM}_i = \sqrt{\frac{1}{\mathbf{n}}\sum_{i=1}^{n}\frac{\left(\mathrm{d}_i^{obs}-\mathbf{F(m)}_i\right)^2}{\left|\mathrm{d}_i^{obs}\right|^2}} \quad (13)$$

is calculated at each iteration, where n is the number of data points. The real and imaginary parts are treated as independent data points to convert the problem into real algebra. A cooling method is used for the regularization parameter as $\lambda_i = \frac{\lambda_{i-1}}{1.5}$. If the value of the objective function increases in any iteration, the update term is damped as, $\mathbf{m}_i = \gamma\mathbf{m}_i + (1-\gamma)\mathbf{m}_{i-1}$, where γ is estimated using a line search approach. For both forward and adjoint responses, the PARDISO direct solver (Schenk and Gärtner, 2004) is used to solve the system matrix.

Numerical Experiments

For testing, the Troll field data recorded along Northern most towline oriented in an East-West direction is presented in this study (see Figure 2 in Gabrielsen et al., 2009). The data consist of an inline electric field recorded at five receivers and 237 sources transmitting 0.25 Hz, 0.75 Hz, and 1.25 Hz frequencies. The subsurface model is discretized for inversion by 200 m and 25 m grid spacing in x- and z-directions, respectively. The coefficient β is set equal to zero. Three strategies for y-grids, viz. 6-, 8-, and 10-grids, are used in this experiment. All the inversion runs converge to a comparable nRMS ($7.40\% \pm 0.01$) after 18 inversion iterations. The vertical and horizontal conductivity images for all three inversion runs are shown in Figure 1 and 2, respectively. All the inversion runs deliver similar subsurface images and recovered resistive anomaly compared well with the gas reservoir, which has its top approximately 1.35 km (Gabrielsen et al., 2009). However, it is observed by thorough examination that the six-grid case shows some degradation in imaging quality. Consequently, the inversion tests illustrate that one may need only 8-10 grids in the y-direction for this algorithm to deliver optimum results.

Development of an efficient 2D MCSEM inversion algorithm

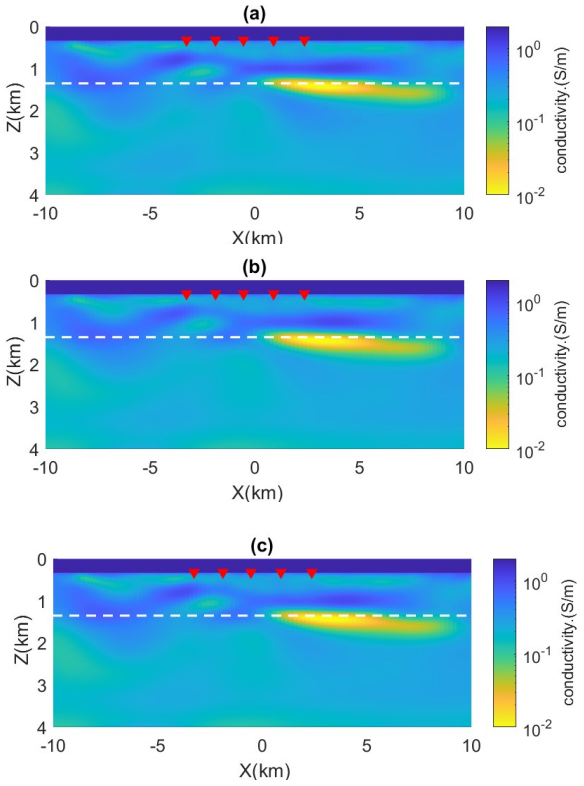

Figure 1: Inverted vertical-conductivity models of Troll field MCSEM data; here, inverted-solid triangles represent the receivers' positions, and a dashed-white line drawn at 1.35 km depicts the top of the gas reservoir; (a) 6 grids; (b) 8 grids; (c) 10 grids.

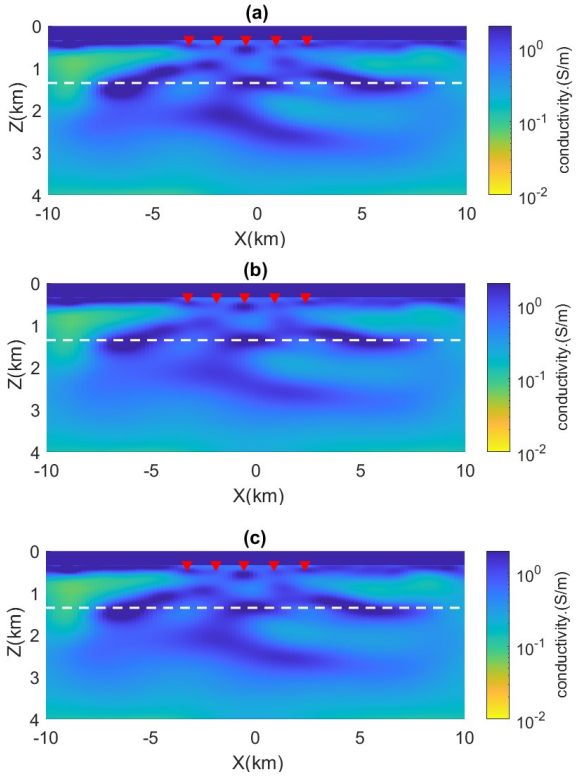

Figure 2: Inverted horizontal-conductivity models of Troll field MCSEM data; here, inverted-solid triangles represent the receivers' positions, and a dashed-white line drawn at 1.35 km depicts the top of the gas reservoir; (a) 6 grids; (b) 8 grids; (c) 10 grids.

A quantitative computation time comparison is unattainable due to the unavailability of a wavenumber-based 2D inversion code to the author. Nevertheless, for eight grids in the strike direction, the non-zero elements of the system matrix will be roughly eight times that in the wavenumber-domain scheme. The proposed scheme will likely be significantly efficient as we require tens of computations in the wavenumber domain followed by inverse Fourier transform for conventional 2D MCSEM modeling. For instance, the MARE2DEM (Key and Ovall, 2011) code solves for at least 30 wavenumbers; consequently, thirty forward problems need to be done in the wavenumber domain, where individual system matrix has one-eighth of non-zero elements than the present code. Again, the computations of all the modeling for a transmitter are necessary to be stored until all the wavenumber calculations for that transmitter are finished because all these are required during the inverse Fourier transform. If the wavenumber-domain simulations are done on separate nodes, all the responses must be transferred to the master node to carry out the inverse Fourier transform. In the present code, all these complications do not occur as the computation is done in the space domain. Furthermore, there is no limitation on the receiver's deviation in strike direction or the prerequisite of projecting the receives onto the transect, which may be required for wavenumber-domain code. For example, in MARE2DEM (Key, 2016), if the along-strike source-receiver offset is large, the choice of wavenumber is advised to be benchmarked using a 1D modeling response. In summary, algorithm development and execution are very straight in the presented algorithm.

Development of an efficient 2D MCSEM inversion algorithm

Conclusion

This study devises an unconventional modeling approach for 2D marine CSEM data where modeling is done in the space domain. The scheme employs boundary conditions derived using field components' symmetric and antisymmetric characteristics for particular transmitter types. The forward modeling is used in an inversion algorithm where the objective function is minimized utilizing a Gauss-Newotn method. The numerical simulations performed using Troll field data reveal that around eight grids are adequate for the strike direction. The scheme is simple to code as it eliminates inverse Fourier transform requirements.

References

Abubakar, A., Habashy, T. M. and V L Druskin, V. L., Knizhnerman, L., and Alumbaugh, D., 2008, 2.5D forward and inverse modeling for interpreting low-frequency electromagnetic measurements. Geophysics, 73:165–177.

Anderson, C., and Mattsson, J., 2010, An integrated approach to marine electromagnetic surveying using a towed streamer and source. First Break, 28, no. 5:71–75.

Christine, C., Samer, N., Kerry, K., and Dan B., 2021, Fluid-rich subducting topography generates anomalous forearc porosity. Nature, 595:255–260.

Constable, S., 2010, Ten years of marine CSEM for hydrocarbon exploration. Geophysics, 75(5):75A67–75A81.

Constable, S., Kannberg, P. K., and Weitemeyer, K., 2016, Vulcan: A deep-towed csem receiver. Geochemistry, Geophysics, Geosystems, 17, no. 2:1042–1064, 2016.

Gabrielsen, P. T., Brevik, I., Mittet, R., and Løseth, L. O., 2009, Investigating the exploration potential for 3D CSEM using a calibration survey over the Troll Field. First Break, 27(6):67–75.

Key, K., 2016, MARE2DEM: a 2-D inversion code for controlled-source electromagnetic and magnetotelluric data. Geophysical Journal International, 207(1): 571–588.

Key, K., and Ovall, J., 2011, A parallel goal-oriented adaptive finite element method for 2.5-d electromagnetic modelling. Geophysical Journal International, 186(1): 137–154.

McGillivray, P. R., Oldenburg, D. W., Ellis, R. G., and Habashy, T. M., 1994, Calculation of sensitivities for the frequency-domain electromagnetic problem. Geophysical Journal International, 116(1):1–4.

Schenk, O., and Gärtner, K., 2004, Solving unsymmetric sparse systems of linear equations with pardiso. Future Generation Computer Systems, 20(3):475–487.

Weiss, C. J., and Constable, S., 2006, Mapping thin resistors and hydrocarbons with marine EM methods, Part II—Modeling and analysis in 3D. Geophysics, 71(6): G321–G332.

Weitemeyer, K., Gao, G., Constable, S., and Alumbaugh, D., 2010, The practical application of 2D inversion to marine controlled-source electromagnetic data. Geophysics, 75(6): F199–F211.